

Study on Surrounding Rock Control Technology of Composite Soft Rock Roadway in Deep Inclined Strata

Yang Yue^{1,a,*}, Gaoshang Wang^{2,b}, Zhiguo Qin^{3,c}, Zhongxin Ji^{4,d}, Tao Wang^{3,e}

¹College of Energy Science and Engineering, Henan Polytechnic University, Jiaozuo, 454001, Henan, China

²Hecheng Coal Mine, Henan Xinmi Hengye Co. Ltd, Xinmi, Henan, 452370, China

³The Ninth Coal Mine of Hebi Coal and Electricity Co., Ltd., Hebi, 458000, Henan, China

⁴Henan Shenhua Coal and Electricity Co., Ltd., Yongcheng, 476600, Henan, China

^aClumsy914@163.com, ^bwanganxin2580@163.com, ^c2109793407@qq.com, ^d305182537qq.com, ^e2099938614@qq.com

*Corresponding author

Abstract: To address the challenge of controlling the deformation of surrounding rock in deep high-stress interlayer tunnels, this study focuses on the engineering background of severe deformation of surrounding rock in a water drainage tunnel of a mine in the 22nd mining area, which traverses multiple layers of inclined soft rock. By employing theoretical analysis and numerical simulations, the research investigates the mechanisms of deformation and failure, as well as the support technologies for interlayer tunnels. The findings include: Under different geological conditions, the vertical stress distribution of roadway surrounding rock shows obvious asymmetric characteristics, and the stress concentration area of left side is more significant than that of right side. Under different geological conditions, the vertical stress distribution of roadway surrounding rock shows obvious asymmetric characteristics, and the stress concentration area of left side is more significant than that of right side. The difference of different rock strata leads to different stress concentration of roadway surrounding rock in different parts. Mudstone and sandy mudstone are weak, which easily leads to stress concentration and surrounding rock damage, and the deformation of roof, floor and shoulder of roadway is more serious. The volume of plastic zone of surrounding rock is significantly affected by the physical and mechanical properties of rock strata. In particular, the existence of soft rock strata will make the surrounding rock of the roadway more prone to plastic flow damage, resulting in the instability of the surrounding rock, and the expansion range of the plastic zone of the roadway is significantly larger. Based on this, a combined support scheme for cross-layer roadway is proposed, which effectively controls the deformation and failure of roadway and improves the overall stability of cross-layer roadway.

Keywords: Deep inclined strata; soft rock; asymmetric deformation; surrounding rock control

1. Introduction

In deep mining, due to the influence of complex geomechanically environment, the morphological characteristics of the excavated roadway in the deformation process are often different from those in the shallow part. A key characteristic is the asymmetric deformation of the surrounding rock in deep roadways^{[1][2]}. According to the practical experience of deep mining, when excavating roadway in inclined rock strata, the deformation on both sides of the roadway, as well as the roof and floor, is often uncoordinated, leading to asymmetric deformation. Moreover, with the damage of the key parts of the roadway, the fracture zone will gradually become larger, causing instability and failure of the surrounding rock, leading to a vicious cycle^[3-6].

Given the asymmetric complex deformation of inclined rock roadways, numerous domestic experts and scholars have conducted theoretical and field studies on the deformation mechanisms and control technologies for these roadways:

In order to solve the problem of asymmetric deformation and instability of surrounding rock after roadway excavation in deep coal seam, Xin^[7] et al. studied the mechanism of this type of damage in

deep rock roadway, and carried out targeted support scheme design. By establishing a physical model, Yang, [8] et al. studied the influence mechanism and deformation mechanism of asymmetric stress on surrounding rock of roadway. Wang [9] et al. studied the problem of asymmetric deformation of deep cross-layer roadway after excavation and support, and proposed asymmetric coupling support measures to strengthen the weak parts. Fan [10] et al. used numerical simulation to study stress distribution and plastic failure areas in surrounding rock of rheological soft rock roadways, proposing an asymmetric support scheme to reinforce large deformation areas. Chen [11] et al. studied and analyzed the mechanism of asymmetric deformation of roadway and its corresponding control methods, and designed an asymmetric coupling support scheme combining anchor net cable spray, grouting and bottom corner bolt. Tian [12] et al. analyzed the characteristics and types of non-uniform pressure stress field by numerical simulation. The deformation and failure mechanisms under different types of non-uniform compressive stress were studied. In order to put forward a new support system of anchor cable jetting deep and shallow hole grouting. Chen [13] et al. identified five typical factors influencing asymmetric deformation: dip angle, burial depth, lithology, lateral pressure coefficient, and aspect ratio. They proposed a method to monitor and record the deformation of the entire roadway section, using surface displacement of surrounding rock as the measurement index. Sun [14] et al. investigated asymmetric deformation and failure of inclined rock roadways, identifying key areas of deformation and proposing asymmetric coupling control measures. Combined with the roadway engineering crossing coal and rock strata, Zhang [15][16] et al. summarized many kinds of uneven failure characteristics such as instability of roadway shoulder, side, floor and whole section, and put forward active closed support forms such as bolt, anchor cable and grouting.

Based on the above research, this paper examines the -800 m drainage roadway of a mine, analyzing the deformation and failure characteristics of cross-layer roadways under varying conditions, revealing their instability mechanisms, and proposing control measures, providing a scientific basis for support decisions in deep high-stress cross-layer roadways.

2. Background of the Project

2.1. Geological overview of roadway

The excavation engineering quantity of -800 m drainage roadway in 22 mining area of a mine is 1082.4 m. It is a long-term drainage service for 22 mining area, with an average buried depth of about 900 m. The geological conditions in the excavation area and surrounding area of the drainage roadway are simple. The stratum strikes southeast and southeast, dips south and southwest, and the dip angle is 12 ~ 14 °. The average dip angle is 13 °. The whole structure is monoclinic structure. The design section of the roadway is a straight wall semi-circular arch, with a net width of 5.2 m and a net height of 4.0 m. Figure 1 is the borehole histogram of -800 m drainage roadway.

rodman shaped	Lamination thickness/m	Rock stratum name
	6.1	Coal seam
	3.11	Sandy mudstone
	2.92	Mudstone(B ₃)
	0.81	L ₁₁ limestone
	0.1	- ₁₉ coal line
	2.05	Mudstone
	0.1	- ₁₈ coal line
	1.78	Sandy mudstone
	1.62	Mudstone
	3.55	L ₉ limestone
	0.2	- ₁₇ coal line
	0.7	Mudstone
	2.75	L ₈ limestone
	2.8	Sandy mudstone
	0.15	- ₁₅ coal line
	2.7	Sandy mudstone
	0.2	- ₁₄ coal line
	1.5	Sandy mudstone
	3.35	L ₇ limestone

Figure 1. Comprehensive histogram of roadway roof and floor

It can be seen from Fig.1 that the roadway passes through the multi-layer soft and hard rock strata during the tunneling process, and the thin coal line, sandy mudstone, mudstone and limestone lithology are common. The lithology of the surrounding rock of the roadway changes greatly, which is not conducive to the stability and support of the roadway, and the roadway is prone to deformation.

2.2. Original supporting way of roadway

The original support form of roadway: anchor net beam + anchor cable + shotcrete combined support. The anchor rod adopts $\phi 22 \times 2600$ mm left-handed non-longitudinal reinforcement rebar high-strength anchor rod, the tray specification is $200 \times 200 \times 12$ mm, and the row spacing is 700×700 mm ; the specification of anchor cable is $\phi 21.6 \times 8000$ mm, 5 in each row, and the spacing between rows is 1400×1400 mm. Full section hanging $\phi 6$ steel mesh ; mesh 100×100 mm ; the ladder beam is made of $\phi 12$ round steel (80 mm wide), arranged horizontally along the roadway, with an interval of 700 mm. The strength grade of shotcrete is C15, and the thickness of shotcrete is 100 mm. The original support scheme of roadway is shown in Figure 2.

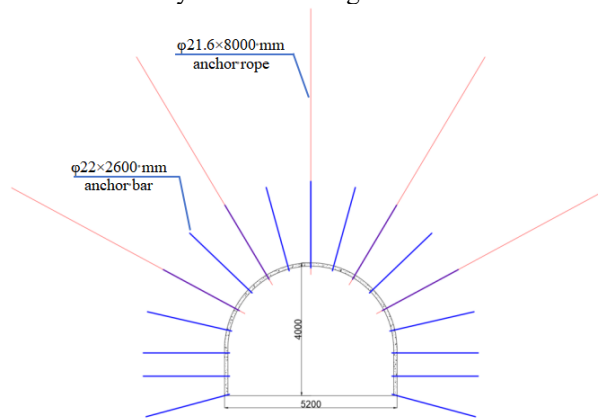


Figure 2. Roadway original support section diagram

3. Numerical Simulation

3.1. Numerical model test scheme

Based on the lithological variation of the cross-section of the -800 m drainage roadway in the 22 mining area and the geological profile of the roadway, the changes in the surrounding rock as it passes through multiple weak rock layers during excavation were modeled. Six test scenarios under different operational conditions are presented in Table 1. FLAC3D numerical simulation software is utilized to evaluate the stress distribution, deformation characteristics of the surrounding rock, and the variations in the plastic zone of the roadway rock under different operational conditions.

Table 1. Scheme different conditions of roadway wear layer

Scheme number	Condition
A1	L9 limestone+Mudstone
A2	L9 limestone+Mudstone+L8 limestone
A3	Mudstone+L8 limestone
A4	Mudstone+L8 limestone+Sandy mudstone
A5	L8 limestone+Sandy mudstone
A6	Sandy mudstone

3.2. Roadway model establishment

The width \times height \times thickness of the numerical calculation model is $50 \text{ m} \times 50 \text{ m} \times 30 \text{ m}$, and the calculation model is shown in figure 3. The average angle of rock strata is 13° . According to the actual situation of the site, the constitutive relationship of the surrounding rock adopts the strain softening model, and the rock mass parameters of the model are assigned. The mechanical parameters of the surrounding rock used in the model are shown in table 2. The initial in-situ stress field : according to the field conditions and the average buried depth of the roadway, the self-weight stress applied above

the calculation model is 22.5 MPa, and the lateral pressure coefficient is 1.0 ; normal displacement constraints are applied to the front, back, left, right, and lower boundaries of the model. To better simulate the actual stress environment of the roadway, a vertical stress gradient is applied in the direction of the vertical stress field.

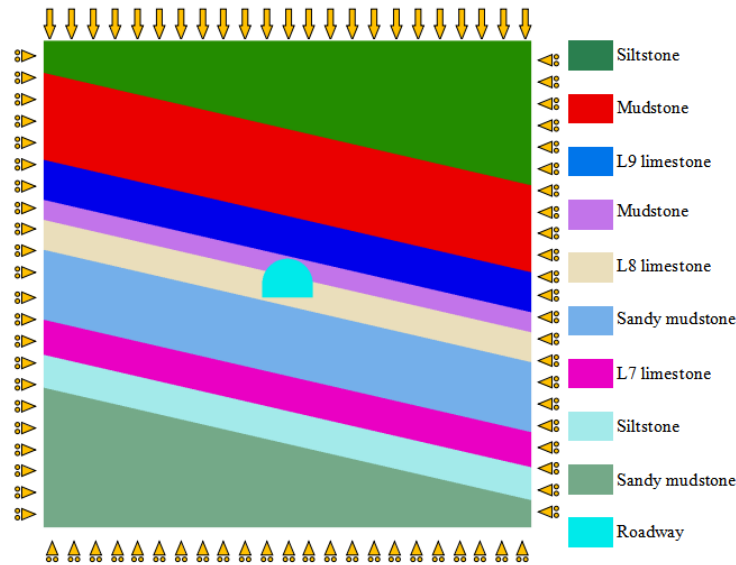


Figure 3. Model and boundary diagram

Table 2. Parameters of blocks

Rock formation	Density kg·m ⁻³	Bulk modulus GPa	Shear modulus GPa	Force of cohesion MPa	Tngle of internal friction	Tensile strength MPa
Limestone	2850	10.9	7.2	21	52	8.6
Mudstone	2350	4.8	2.0	2.4	24	0.7
Sandy mudstone	2470	5.5	4.1	2.3	23	0.7
Siltstone	2450	6.3	3.5	2.6	24	2.1
Coal seam	1440	4.5	1.7	1.8	25	0.5

4. Analysis of Numerical Test Results

To investigate the deformation, failure modes, and plastic zone evolution during roadway crossing, monitoring lines, each 20 meters long, were positioned perpendicular to the roof, floor, sides, and shoulders. Forty-one monitoring points were distributed across various locations to measure displacement and plastic zone depth, with the objective of uncovering the changes in stress distribution, deformation, and plastic zone of the surrounding rock post-excavation.

4.1. Stress distribution law of surrounding rock of roadway

After the roadway excavation, without support, the vertical stress distribution characteristics of the surrounding rock in the inclined composite soft rock roadway under various working conditions are shown in Figure 4. As seen from the figure, stress around the roadway decreases to varying extents after excavation without support. The peak vertical stress concentration in the surrounding rock occurs at the roadway sides, exhibiting a distinct asymmetric distribution. The stress peak and concentration area on the right side are larger than those on the left, with the stress concentration area on the left extending further towards the side than on the right.

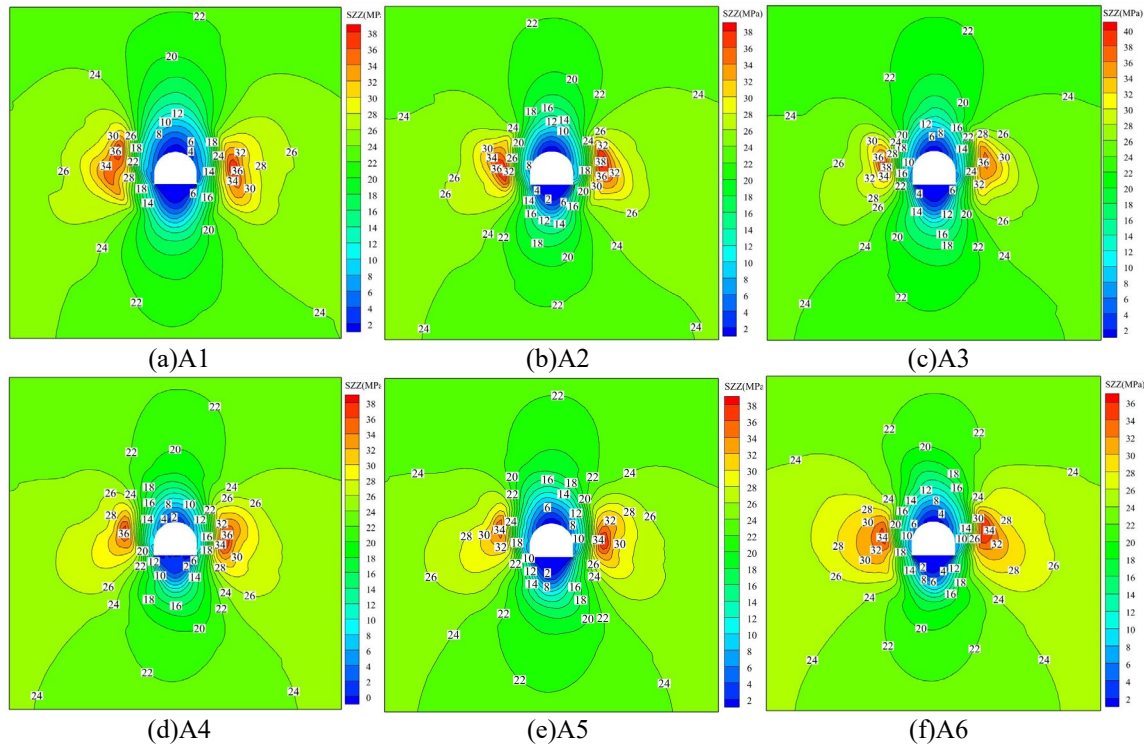
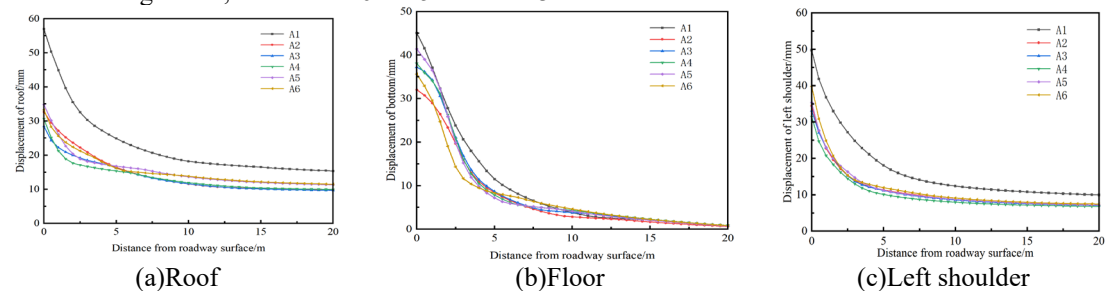


Figure 4. Vertical stress cloud diagram of roadway surrounding rock under different working conditions

The vertical stress distribution of roadway surrounding rock in six different working conditions shows that the stress concentration phenomenon of roadway side is significant. When mudstone and sandy mudstone are the main lithology of the two sides, the stress concentration degree is large in the range of the left and right sides, and the maximum vertical stress of the left side is 36 MPa, the maximum vertical stress on the right side is 38 MPa. When limestone is the predominant lithology on both sides, the stress concentration decreases relative to mudstone and sandy mudstone. In this case, the maximum vertical stress is 34 MPa on the left side and 36 MPa on the right side. This phenomenon suggests that mudstone and sandy mudstone strata are weak and more prone to failure under stress, leading to a decrease in bearing capacity. The peak stress is transferred to the deeper surrounding rock, where it is crushed, releasing stress and slightly reducing stress concentration. The stronger limestone can withstand greater ground stress, leading to higher stress concentration. In summary, the lithological differences between rock strata in the roadway result in the asymmetric distribution of vertical stress.

4.2. Stress distribution law of surrounding rock of roadway

As shown in Figure 5, the varying rock strata in the roadway under different working conditions lead to inconsistent deformation patterns of the surrounding rock in different sections of the roadway. The roof displacement in conditions A1 to A6 follows the order: A1 > A5 > A6 > A2 > A4 > A3. For the bottom plate, the displacement sequence is A1 > A5 > A4 > A3 > A6 > A2. The left shoulder displacement ranks as A1 > A6 > A5 > A2 > A3 > A4, while the right shoulder displacement is A1 > A6 > A2 > A5 > A3 > A4. On the left side, the displacement follows A1 > A6 > A5 > A4 > A2 > A3, and on the right side, it is A1 > A6 > A5 > A2 > A3 > A4.



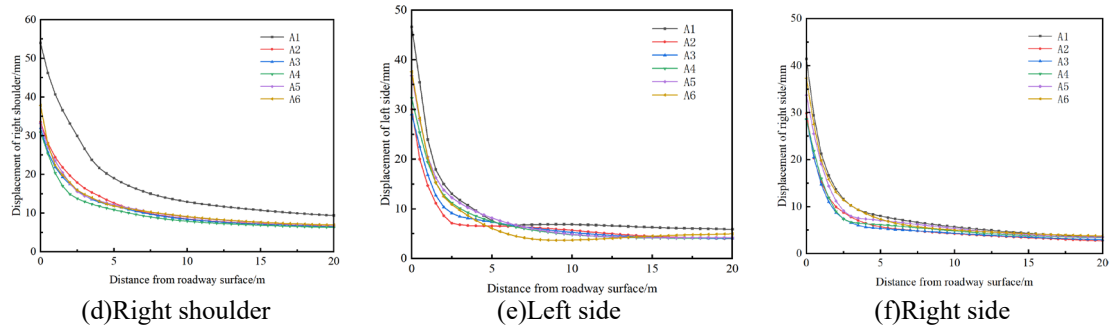


Figure 5. Displacement curve of crossing roadway under different working conditions

Based on the comparison and analysis of the above data, and considering the displacement of the roadway roof, floor, sides, and shoulders, the working conditions A1 to A6 are categorized into two groups, with the roadway roof as the example. The first group, A1, exhibits significant deformation, with roof displacement exceeding 50 mm. The second group, consisting of A2, A3, A4, A5, and A6, shows minor deformation, with roof displacement below 35 mm. The primary reasons are as follows: The roof of the first type of roadway consists of mudstone, which has low strength and weak bearing capacity, leading to significant deformation of the roof. Analysis of the roadway stratum histogram reveals that mudstone is prone to swelling, which further reduces its strength. As a result, the roadway roof becomes the weakest part of the surrounding rock's bearing structure. The roof of the second type of roadway is composed of limestone, which has high strength and bearing capacity, resulting in minimal deformation compared to other working conditions.

4.3. Distribution of plastic zone of roadway surrounding rock

Figure 6 illustrates the evolution of the plastic zone in the surrounding rock during roadway penetration. The surrounding rock of the roadway primarily experiences shear failure, with tensile failure occurring less frequently. When tensile failure does occur, it is mainly concentrated in the shallow surrounding rock. The plastic failure zone in the surrounding rock of the roadway is primarily located in the low-strength mudstone and sandy mudstone, with a large expansion range. In contrast, the plastic failure zone in the high-strength limestone has a smaller expansion range. The plastic failure zone in the surrounding rock of the roadway is primarily located in the low-strength mudstone and sandy mudstone, with a large expansion range. In contrast, the plastic failure zone in the high-strength limestone has a smaller expansion range.

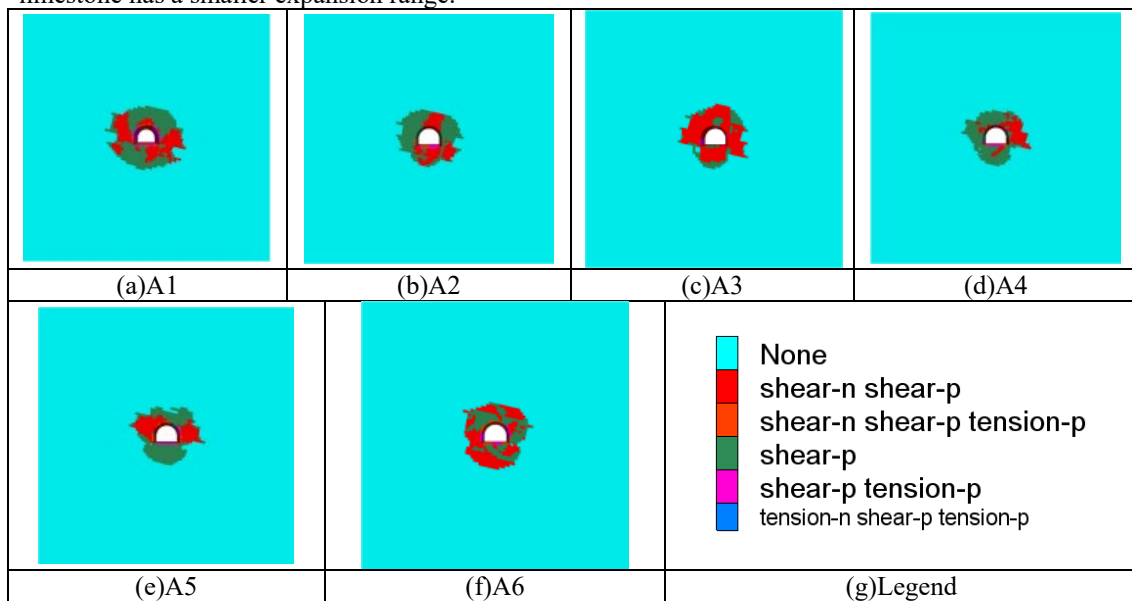


Figure 6. Plastic zone of roadway surrounding rock under different working conditions

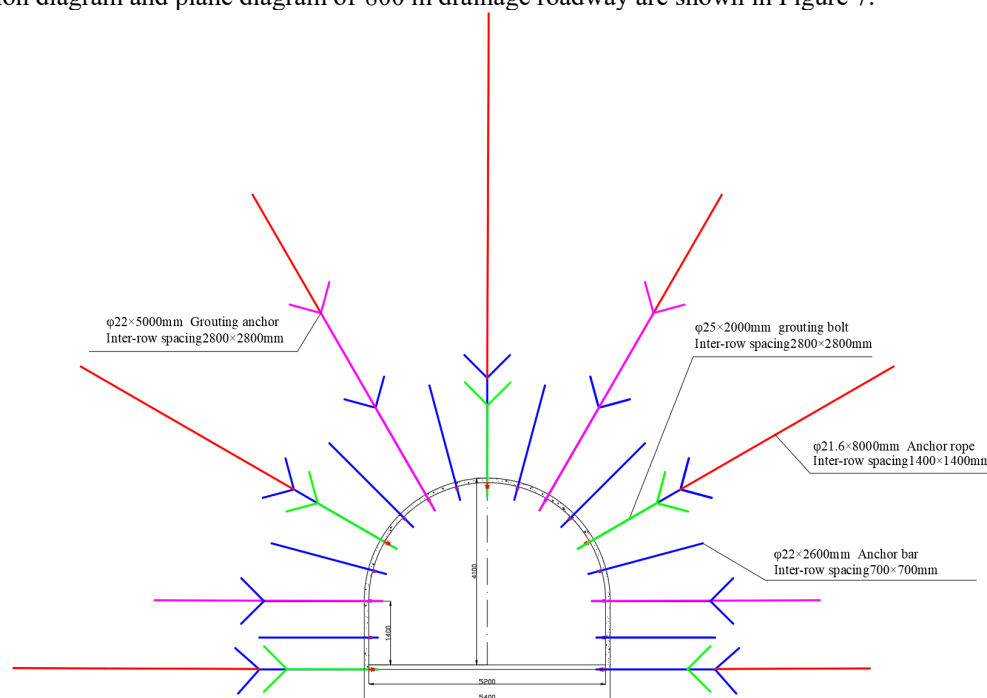
Comparing the distribution of the plastic zone in the roadway sections under six different working conditions, the variation in the plastic zone of the surrounding rock is inconsistent. The volume of the plastic zone follows the order: A1 > A6 > A3 > A5 > A2 > A4. The plastic zone in the surrounding rock

of the roadway is primarily characterized by tensile-shear failure, mainly due to the transition of the shallow surrounding rock from a unidirectional to a bidirectional force state. However, the overall failure is primarily characterized by compression-shear failure, with a larger plastic zone under high-stress conditions. During roadway excavation, the interaction between soft and hard rocks results in an asymmetrical distribution of the plastic zone. The plastic zone at the soft-hard rock interface shows abrupt changes. As the plastic zone transitions from hard rock to soft rock, it becomes more evenly distributed and expands significantly. As the plastic zone transitions from soft rock to hard rock, it narrows, and its expansion range decreases. In general, the plastic zone in soft rock exhibits a larger expansion range, whereas in hard rock, the range is smaller.

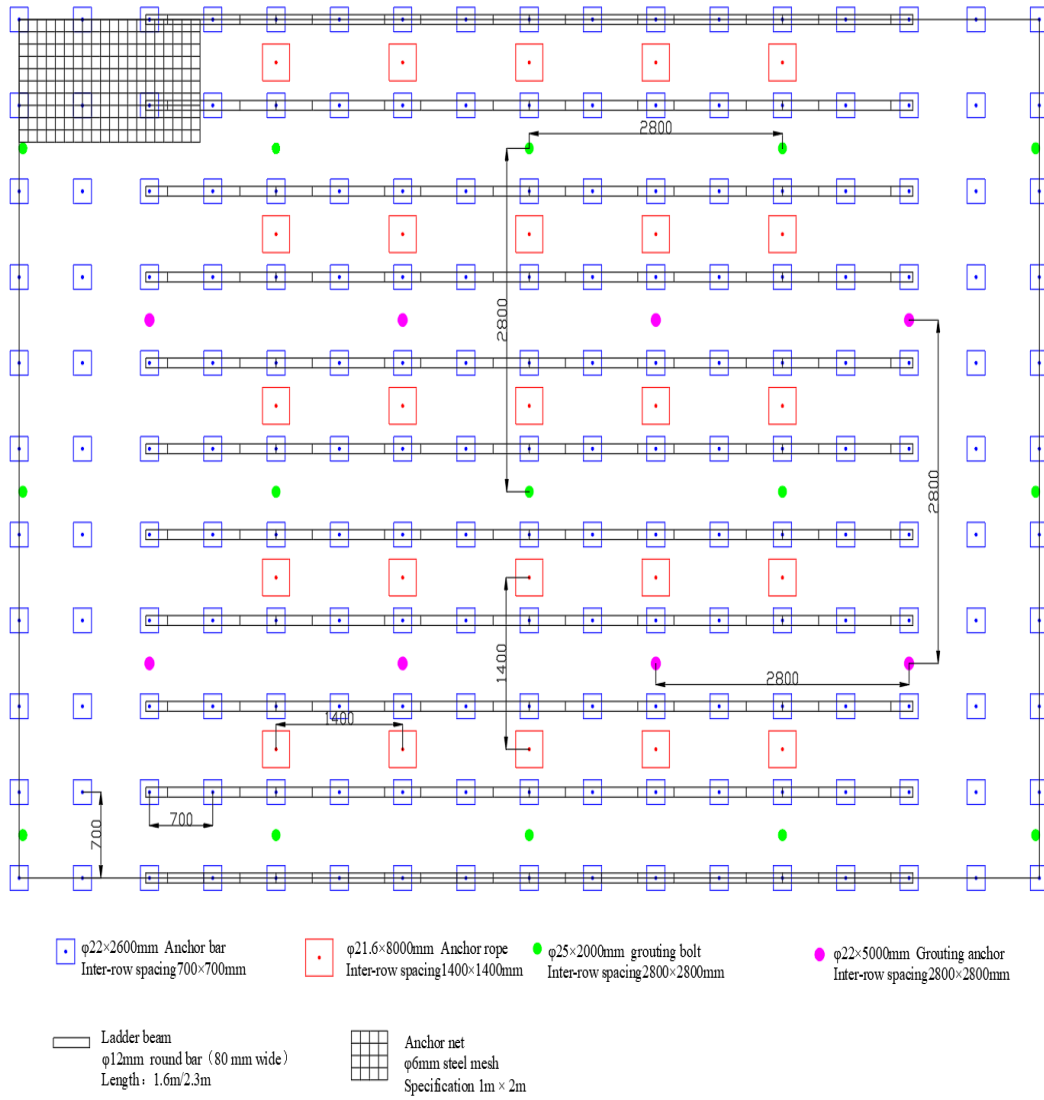
5. Deformation control countermeasures of cross-layer roadway

Given the asymmetric deformation characteristics of deep, gently inclined soft rock roadways, various support structures should not be merely superimposed. Instead, the full potential of each support structure should be utilized to ensure the stability of the surrounding rock and achieve effective coupling between the roadway rock and the support system.

According to the deformation and failure mechanism of -800 m drainage roadway, a step-by-step combined support scheme of " anchor net spray + anchor cable + shotcrete + wall back grouting " is proposed. The anchor rod adopts $\phi 22 \times 2600$ mm left-handed non-longitudinal reinforcement rebar high-strength anchor rod with 700×700 mm row spacing. Each anchor rod uses one roll of MSK2550 and MSZ2550 anchoring agent for end anchoring, and the tray specification is $200 \times 200 \times 12$ mm. $\phi 6$ mm steel mesh, specification 1000×2000 mm ; the reinforced ladder beam is made of $\phi 12$ mm round steel (80 mm wide) and is arranged horizontally along the roof of the roadway. The anchor cable adopts $\phi 21.6 \times 8000$ mm steel strand, 5 rows of anchor cables are evenly arranged along the roof, and the row spacing between the anchor cables is 1400×1400 mm. Each anchor cable is anchored with a roll of MSK2550 and three rolls of MSZ2550 anchoring agent, and the anchor cable tray specification is $300 \times 300 \times 20$ mm. Spraying C15 concrete, spraying thickness 100 mm and meet the requirements of grouting ; the grouting behind the wall adopts graded grouting. The first grouting adopts $\phi 25 \times 2000$ mm grouting bolt, and the second grouting adopts $\phi 22 \times 5000$ mm grouting anchor cable. The row spacing is 2800×2800 mm, and the two grouting adopts fork arrangement. Grouting with 425 # cement or superfine cement, water cement ratio (mass ratio) : $1.1 \sim 1.4 : 1$; the grouting pressure reaches 4 MPa, and the grouting sequence is from the lower part of the roadway to the vault. The first grouting can be delayed by 90 m, and the second grouting can be delayed by 120 m. The support section diagram and plane diagram of -800 m drainage roadway are shown in Figure 7.



(a) Support section diagram



(b) Support plane diagram

Figure 7. -800m drainage roadway support section and plan

6. Control effect analysis

The combined support technology is applied in the large-section intersection of the upper roadway. A surface displacement monitoring station is installed in the roadway, and the deformation monitoring results are shown in Figure 8.

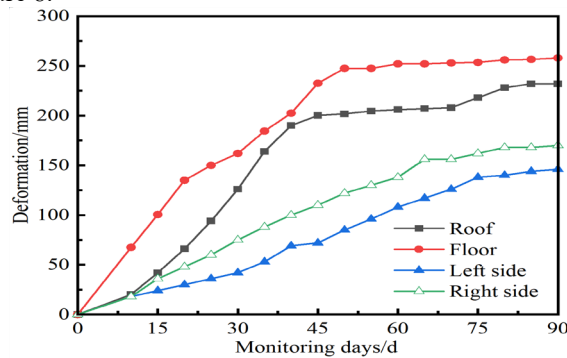


Figure 8. Roadway deformation displacement monitoring curve

After 90 days of roadway support, the roof subsidence of the roadway is 232 mm, the floor heave is 258 mm, the internal extrusion of the left side is 146 mm, and the internal extrusion of the right side is

170 mm.

Following the implementation of the control scheme, the roadway underwent a process of "rapid deformation → stabilization." After excavation, the roadway experienced floor heave, roof subsidence, and side deformation. Between 40 and 50 days of support, the deformation rate of the surrounding rock slowed and gradually stabilized. At this point, the surrounding rock stress had been transferred to the deeper stable rock mass, ensuring the roadway's stability.

7. Conclusion

(1) The variation in surrounding rock across different parts of the cross-layer roadway results in inhomogeneous and asymmetric deformation and failure, causing uncoupling between the support components and surrounding rock, which affects overall stability. The interface between soft and hard rocks primarily undergoes shear deformation failure, while tensile failure occurs less frequently and is mainly concentrated in the shallow surrounding rock.

(2) The plastic failure zone in the cross-layer roadway is primarily found in soft rock, which has lower strength and a larger expansion range, while the plastic failure zone in harder rock is smaller. At the interface between soft and hard rocks, the plastic failure zone increases along the interface, resulting in a non-uniform distribution of plastic failure within the roadway.

(3) A combined support scheme for cross-layer roadways is proposed to effectively control large deformations and failures, thereby enhancing overall roadway stability.

References

- [1] Yuan Liang, Xue Junhua, Liu Quansheng, et al. Surrounding rock stability control theory and support technique in deep rock roadway for coal mine[J]. *Journal of China Coal Society*, 2011, 36(4): 535-543.
- [2] Pan Rui, Wang Qi, Jiang Bei, et al. Failure of bolt support and experimental study on the parameters of bolt-grouting for supporting the roadways in deep coal seam[J]. *Engineering Failure Analysis*, 2017, 80: 218-233.
- [3] Wang Qi, Ran Rui, Jiang Bei, et al. Study on failure mechanism of roadway with soft rock in deep coal mine and confined concrete support system[J]. *Engineering Failure Analysis*, 2017, 81: 155-177.
- [4] Wang Lei, Wang Qi, Li Shucui, et al. Stability analysis and characteristic of seismic activity during roadway development in soft rock[J]. *Journal of Mining & Safety Engineering*, 2018, 35(1): 10-18.
- [5] Wang Xiangyu, Bai Jianbiao, Wang Meng. Study on asymmetric instability mechanism and control technology for roadway in deep inclined rock strata with weak plane[J]. *Journal of Mining & Safety Engineering*, 2015, 32(4): 544-551.
- [6] Yang Fan, Chen Weizhong, Zheng Pengqiang, et al. Research on mechanism of deformation and failure for steeply incline roadways in soft-hard alternant strata and its support technology[J]. *Rock and Soil Mechanics*, 2021, 35(8): 2367-2374.
- [7] Xin Guangming, Yuan Qi, Zheng Yongsheng, et al. Asymmetric Deformation Mechanism and Control Technology in Deep Roadway[J]. *Safety in Coal Mines*, 2020, 51(3): 207-210, 215.
- [8] Yang Xiaojie, Ming Wei, Zhang Weiran, et al. Support on Deformation Failure of Layered Soft Rock Tunnel Under Asymmetric Stress[J]. *Rock Mechanics and Rock Engineering*, 2022, 55(12): 7587-7609.
- [9] Wang Jiong, Guo Zhibiao, Cai Feng, et al. Study on the asymmetric deformation mechanism and control countermeasures of deep layers roadway[J]. *Journal of Mining & Safety Engineering*, 2014, 31(1): 28-33.
- [10] Fan Ziyi, Li Yongliang, Sun Hao, et al. Characteristics and control measures of unsymmetric deformation of roadways within weakly-cemented soft rock[J]. *Journal of Mining and Strata Control Engineering*, 2022, 4(2): 44-53.
- [11] Chen Shangyuan, Song Changsheng, Guo Zhibiao, et al. Asymmetric deformation mechanical mechanism and control countermeasure for deep roadway affected by mining[J]. *Journal of China Coal Society*, 2016, 41(1): 246-254.
- [12] Maolin Tian, Lijun Han, Xuxu Yang, et al. Asymmetric deformation failure mechanism and support technology of roadways under non-uniform pressure from a mining disturbance[J]. *Bulletin of Engineering Geology and the Environment*, 2022, 81(5): 56-61.
- [13] Yuxue Chen, Liping Li, Zongqing Zhou, et al. Asymmetric deformation characteristics and support

scheme design of the surrounding rock in deep roadway[J]. Arabian Journal of Geosciences, 2021, 14(7): 1-20.

[14] Sun Xiaoming, Zhang Guofeng, Cai Feng, et al. *Asymmetric deformation mechanism within inclined rock strata induced by excavation in deep roadway and its controlling countermeasures[J]. Chinese Journal of Rock Mechanics and Engineering, 2009, 28(6): 1137-1143.*

[15] Zhang Nong, Li Baoyu, Li Guichen, et al. *Inhomogeneous damage and sealing support of roadways through thin bedded coal-rock crossovers[J]. Journal of Mining & Safety Engineering, 2013, 30(1): 1-6.*

[16] Zhang Nong, Li Guichen, Xu Xingliang. *Argillation of a roof weak interlayer due to water seepage and its influence on roadway stability[J]. Journal of China University of Mining & Technology, 2009, 38(6): 757-763.*